

## **Air-Ice-Ocean Coupling During a Strong Mid-Winter Cyclone, Part 1: Observing Coupled Dynamic Interactions Across Scales**

**D. M. Watkins<sup>1</sup>, P. O. G. Persson<sup>2</sup>, T. Stanton<sup>3</sup>, A. Solomon<sup>2</sup>, J. K. Hutchings<sup>4</sup> J. Haapala<sup>5</sup>, G. Svensson<sup>6</sup>**

<sup>1</sup>Center for Fluid Mechanics, Brown University, Providence, RI, USA. <sup>2</sup>Cooperative Institute for Research in Environmental Sciences, University of Colorado, Boulder CO and NOAA/Physical Sciences Laboratory, Boulder CO, USA. <sup>3</sup>Moss Landing Marine Laboratories and Naval Postgraduate School, CA, USA. <sup>4</sup>College of Earth Ocean and Atmospheric Sciences, Oregon State University, Corvallis, OR, USA. <sup>5</sup>Finnish Meteorological Institute, Helsinki, Finland. <sup>6</sup>Stockholm University, Stockholm, Sweden

Corresponding author: Daniel Watkins ([daniel\\_watkins@brown.edu](mailto:daniel_watkins@brown.edu))

### **Contents of this file**

Figures S1 to S4

Table S1 to S2

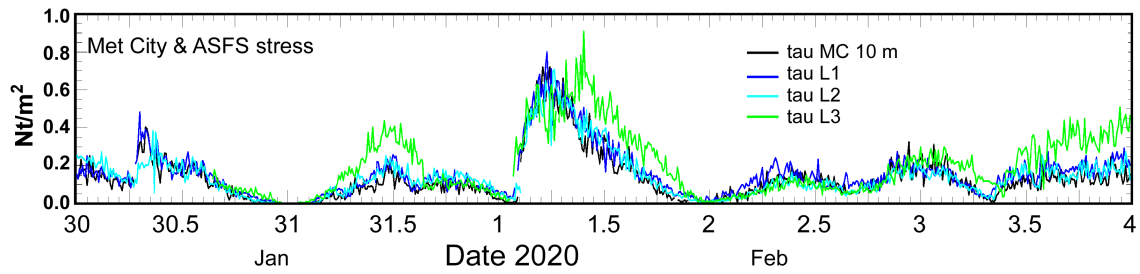
### **Introduction**

Figure S1 shows the stress measurements at the CO and L sites as an extension of the data shown in Figure 5. Figure S2 shows the deformation in the Distributed Network for comparison with Figure 10. Figure S3 shows the larger-scale deformation for comparison with Figure 9. Figure S4 includes the buoy velocity components and wind speed map for comparison with Figure 8.

Table S1 lists the instruments and variables used in the study. Table S2 lists the reference buoys used at multi-sensor sites.

In addition, we include 5 animations. Animations `fig09_animation.mp4`, `fig10_animation.mp4`, `figS2_animation.mp4`, and `figS3_animation.mp4` are useful for comparison with the corresponding figures, so that maps at hourly resolution can be

easily accessed. The animation radar\_animation.mp4 is a timelapse of the 15-min resolution ice radar data.



**Figure S1.** Stress measurements from the 3 ASFS stations.

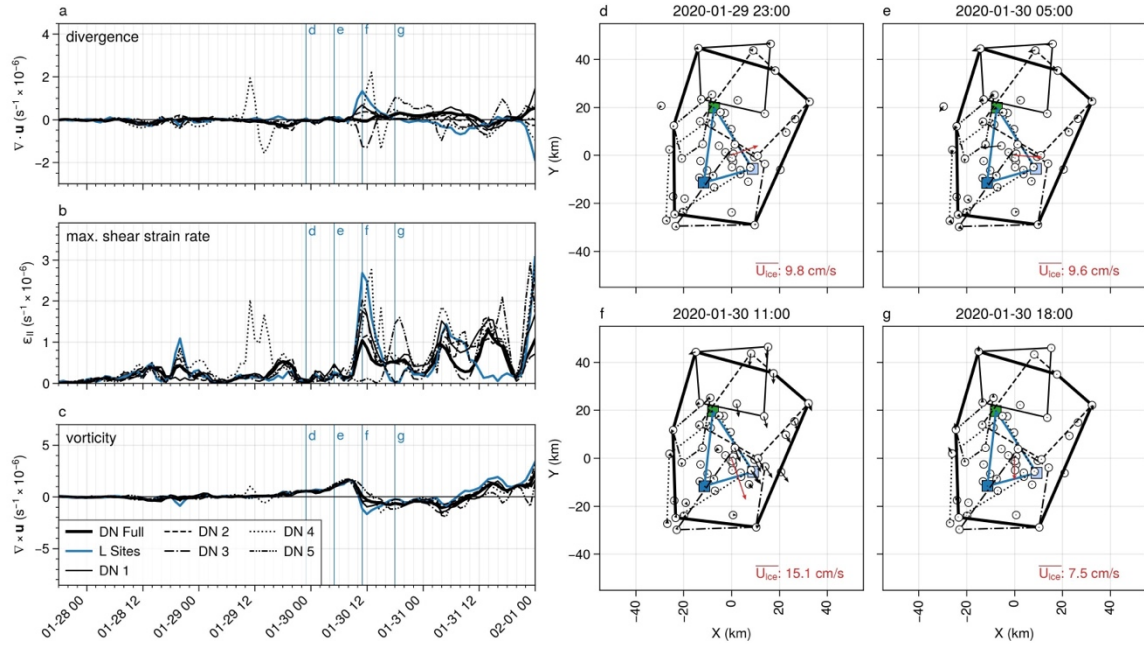


**Figure S2.** Strain rate components (a-c) and velocity anomalies (d-g) of the Distributed Network for the Jan 30 cyclone. Polygons used for the deformation calculations are shown in panels d-g. The polygons were selected manually; note that the buoy in the upper left was not included in the “DN Full” array due to periods of missing data. Velocity anomalies in panels d-g were computed relative to the ensemble average velocity, which is shown as the red arrow at the center of each panel.

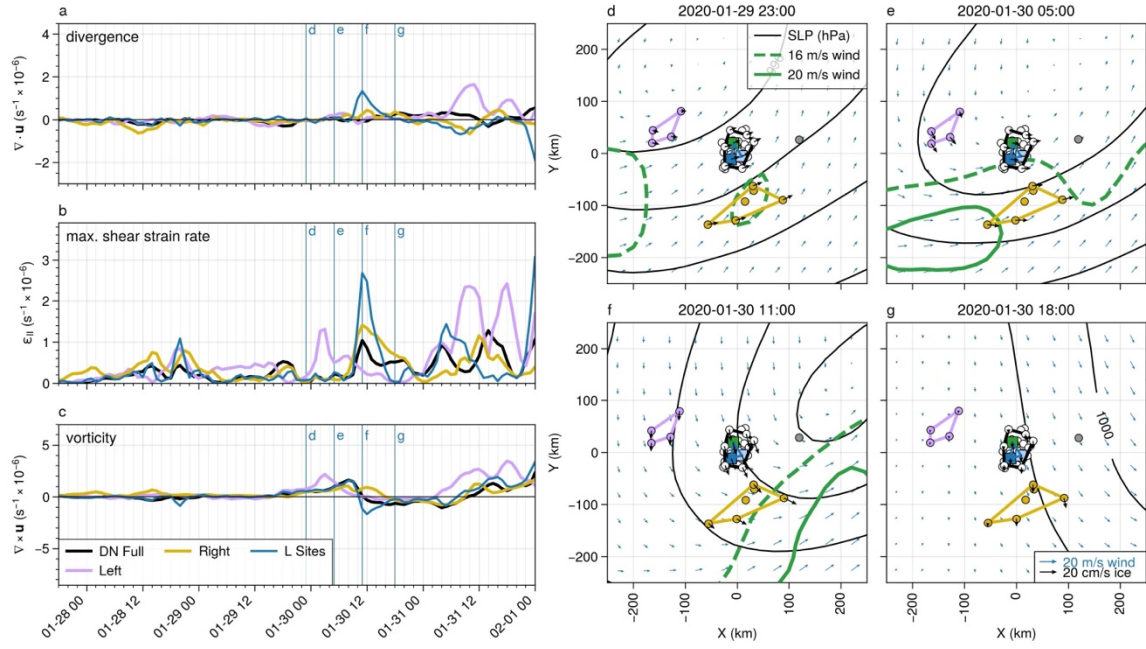


**Figure S3.** Strain rate components (a-c) and ice and wind velocities (d-g) of the Extended Distributed Network for the Jan 30 cyclone. Polygons used for the deformation calculations are shown in panels d-g.

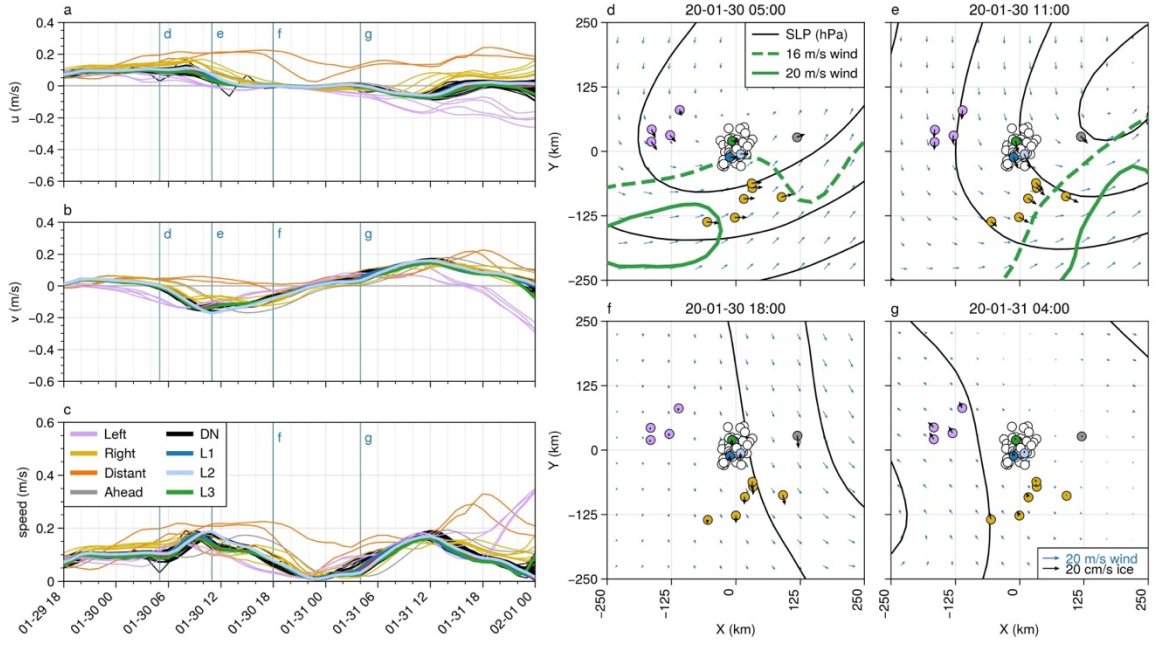


**Figure S4.** Left: Buoy velocity components (a, b) and magnitude (c) for the period from 18 UTC on 29 January to 0 UTC on 1 February. The top and middle panels show the  $u$  and  $v$  velocity components relative to the north polar stereographic projection, thus corresponding to the  $x$  and  $y$  axis, respectively, in the panels on the right. For the period shown here, the positive  $y$  direction is approximately northward. Right: Snapshots of buoy motion (thick black arrows) superimposed on the ERA5 sea level pressure isobars (black contours, 4 hPa spacing) and near-surface (10 m) wind fields (blue arrows) at times corresponding to vertical lines in the velocity time series to the left.

Site	Instrument	Measurements	Reference
CO (Polarstern)	Rawinsonde	Temperature Humidity Horizontal winds	Shupe et al., 2022
	Vertically-pointing Ka-band radar	Radar reflectivity Radial velocity	
	Sea ice radar (X-band)	Radar reflectivity	Hessner et al., 2019, Krumpen et al., 2021a
	Conductivity, temperature, depth (CTD) sampling	Salinity Temperature	Rabe et al., 2022
CO (Met City)	Met Tower	Temperature Humidity Pressure 4-component broadband radiative fluxes 3D Wind	Shupe et al., 2022
	Acoustic Doppler Current Profiler	Currents	Rabe et al., 2022
	SIMBA	Ice thickness	Rabe et al., 2024
	SIMB3	Ice thickness	Perovich et al., 2023
	Autonomous Ocean Flux Buoy (AOFB)	Temperature Salinity 3D currents	Stanton et al., 2012, Rabe et al., 2024, Rabe et al., 2022
L-sites	Atmospheric Surface Flux Stations (ASFS)	Temperature Humidity Pressure 4-component broadband radiative fluxes 3D Wind	Cox et al., 2023
	SIMBA	Ice thickness	Rabe et al., 2024
	SIMB3	Ice thickness	Perovich et al., 2023
P-sites	GPS buoys	Position	Bliss et al., 2023

**Table S1.** Instruments described in Section 2.

Site	Sensor ID
CO	2019T66
L1	2019T67
L2	2019T65
L3	2019S94
M1	2019O1
M2	2019V2
M3	2019O3
M4	2019O4
M5	2019O5
M6	2019O6
M8	2019T69
<b>Table S1</b>	

**Table S2.** Representative buoys for multi-sensor sites